Scattering in an Amorphous Layer Measured by Dechanneling*

S. U. Campisano, G. Foti, F. Grasso, and E. Rimini
Istituto di Struttura della Materia dell'Università di Catania, Corso Italia 57, I95129 Catania, Italy
(Received 19 December 1972)

Channeling experiments by proton backscattering have been made along the ⟨ 111 ⟩ axis of silicon crystals covered with aluminum and gold layers to investigate the depth dependence of the dechanneled fraction on crystal temperature (80–300 °K), beam energy (0.6–1.5 MeV), and film thickness (100–4000 Å). The dechanneled fractions $\chi(z)$ have been compared with calculated values obtained by two different procedures. (i)The changes with depth in the transverse energy of a channeled particle due to crystal scattering have been described by the steady-increase approximation and a maximum allowed transverse energy, related to the experimental critical angle, was assumed for a channeled particle. The adopted angular distribution of beam particles just beneath the crystal surface accounted for both the scattering in the amorphous surface layer and through the crystal surface. (ii) Alternatively, $\chi(z)$ has been obtained by convolution of the angular distribution of particles scattered only in the amorphous surface layer with the experimental channeling angular-yield profile measured in an uncovered crystal. Both procedures give good agreement with experiments, thus supporting the steady-increase approximation for the crystal scattering and Meyer's treatment for the amorphous scattering. As a prelude to measurements in heavily damaged crystals, these approaches have been reversed, so that the distribution of scattered particles and then the thickness of the amorphous layer have been obtained by dechanneled-fraction measurements. The extension of the method to the case of small defect concentration in a nearly perfect crystal is briefly discussed.

I. INTRODUCTION

Channeling measurements, being sensitive to lattice imperfections, have been used to determine lattice disorder in ion-implanted[1] samples and in epitaxially grown single crystals.[2] The disorder profiles inside the crystal could be obtained, in principle, by a suitable analysis of measured dechanneled fraction versus penetration, and a few efforts along this line have been reported.[3]

In a perfect crystal, however, the dechanneling can be described analytically[4] in terms of elementary scattering processes,[5] taking into account (a) the initial angular distribution of particles just beneath the crystal surface, (b) the interaction with electrons and vibrating nuclei in the channel, and (c) transitions from the aligned to the random component of the beam.

It seems useful to extend this approach to damaged crystals. A preliminary classification can be made as a function of the defect concentration; (i) very high defect concentration which destroys the crystal lattice within a well-defined layer, thus producing a quasiamorphous film; (ii) low concentration of defects in a nearly perfect crystal. In the former, defects modify only the angular distribution of the particles impinging on the underlying perfect crystal, while in the latter the scattering of a channeled particle by a defect occurs simultaneously with other scattering processes present in the undamaged crystal (processes depending upon lattice vibrations and the electron distribution).

In the present work we consider the heavily damaged case, which has been simulated by a thin evaporated layer on the crystal surface. It must be remarked that this case is the simpler one, and it allows a more direct extension of the approach developed for perfect crystals.

As was recently pointed out,[6] the comparison between experimental and calculated dechanneled fraction for covered crystals gives a direct test of the approximations involved in the dechanneling treatment because the beam spreading introduced by the layer increases the measured yield by an order of magnitude with respect to an uncovered sample, thus increasing the experimental sensitivity. A detailed investigation of the importance of the different approximations has been performed, taking advantage of the dechanneled-fraction dependence on beam species and energy, on crystal temperature, and on the amorphous-layer thickness.

Minimum-yield measurements give information on the condition for particle transition from the aligned to the random beam (dechanneling condition). The minimum yield χ_0 is given in fact by the integral of the particle angular distribution just beneath the crystal surface weighted over the transition probability. Usually one assumes that a particle belongs to the random component of the beam when its angle with the channel axis is greater than $\psi_{1/2}$, the experimental critical angle for channeling. It is obvious that the transition probability is more sophisticated than this step-function approximation, being even closer to the rounded

experimental angular-yield profile or, as recently proposed, [7] to its azimuthal average.

These aspects concerning the transition probability have been detailed; the influence of the crystal surface due to the channel potential (transmission factor) on the initial angular distribution have been also taken into account to calculate minimum yield. This has been done with the aim of bringing to light when it is possible to adopt the simplest procedure which implies (i) a step function for dechanneling condition and (ii) the initial distribution of the particles as determined by the scattering in the amorphous layer neglecting the transmission factor. The angular distribution of particles after traversing the film has been calculated according to the Meyer[8] treatment of plural scattering which has been verified by transmission measurements[9,10] and by channeling experiments.[6,7]

Because the initial distribution and the dechanneling condition are known from minimum-yield investigations, the depth dependence of the dechanneled fraction $\chi(z)$ gives information on the scattering experienced by a channeled particle. This scattering, which increases the angle the particle trajectory forms with the channel axis and hence the particle transverse energy, is due to thermal vibrations of the crystal nuclei and to the electron distribution in the channel. It has been shown that, neglecting diffusion, [11] the changes in transverse energy can be obtained analytically[4,12] (steady-increase approximation). This approximation, the initial distribution, and the aligned-to-random transition criterion examined by the χ_0 measurements allow the calculation of the depth dependence of the dechanneled fraction to be compared with experiments.

An alternative procedure to determine $\chi(z)$ in a covered crystal is provided by convolution of the scattered particle distribution in the amorphous layer with the experimental angular yield profile measured at the corresponding depth z in an uncovered crystal. This treatment does not imply any assumption because the yields include both the scattering through the crystal surface and the aligned-to-random transition. The agreement found between the experiments and the dechanneled fractions calculated by convolution further supports Meyer's treatment of plural scattering.

The procedures adopted to compute the depth dependence of dechanneled fraction have been reversed, on the basis of the agreement found throughout. This has been done with the aim of determining from the measured dechanneled fraction the angular distribution of scattered particles.

This investigation seems a preliminary and essential step to determine disorder by dechanneled fraction measurements in heavy damaged crystals.

All the above points have been investigated by experiments carried out on silicon crystals covered with aluminum and gold films. The film thickness has been chosen so that the average number of scattering processes within the screening distance ranged between 1 and 10, as it occurs typically in a damaged crystal. The choice of protons as a probe beam allowed sampling to large depth and made available a wide range of values for the comparison between experiments and theory.

II. EXPERIMENTAL

Measurements have been performed by the backscattering technique using a collimated beam of protons. The apparatus consists of the 2.5-MeV Van de Graaff accelerator, and of a goniometric scattering chamber maintained at 10^{-6} Torr. The proton beam was collimated within ± 0.5 mrad by means of an arrangement of circular apertures; the target could be oriented with the same accuracy. Particles backscattered from the target through a laboratory angle of 150° were detected by a 25-mm^2 surface-barrier detector, 8 cm from the target. Standard electronics were used to feed pulses to a 4096-channel pulse-height analyzer. The energy resolution of the system was 10-keV full width at half-maximum (FWHM) for 1-MeV protons. The beam energy ranged between 0.6 and 1.5 MeV; the temperature of the crystal, in the thermal contact with a thermostatic bath, was set at either 80 or 300 °K. A more detailed description of the setup has been previously reported.[4]

The samples were prepared by vacuum deposition of different thicknesses of Al and Au layers onto silicon substrates at room temperature. The same technique previously adopted[6] has been used to mask the crystal during the evaporation, thus allowing an uncovered part of Si to remain. The sample was initially aligned along a major axis in the uncovered part and then the incident beam was translated to various portions of the target for a direct comparison of the yield. Misalignment during beam translation performed by means of mobile apertures has been measured by comparing the angular-yield profiles and it is of the same order of the beam collimation. Comparison between Au signals obtained by backscattering of He^+ for different angles of incidence shows no ordered structure in the evaporated layer. Beam translation has been used to test the uniformity of film thickness and no significant variation has been detected within the resolution limit.

Film thicknesses ranged between 100 and 600 Å for Au and between 1000 and 4000 Å for Al. The number of Al and Au atoms per cm^2 was determined[13] by helium backscattering and it was converted into Å's with the following factor: 1 Å = 5.9×10^{14} Au atoms/cm^2 and 6.0×10^{14} Al atoms/cm^2,

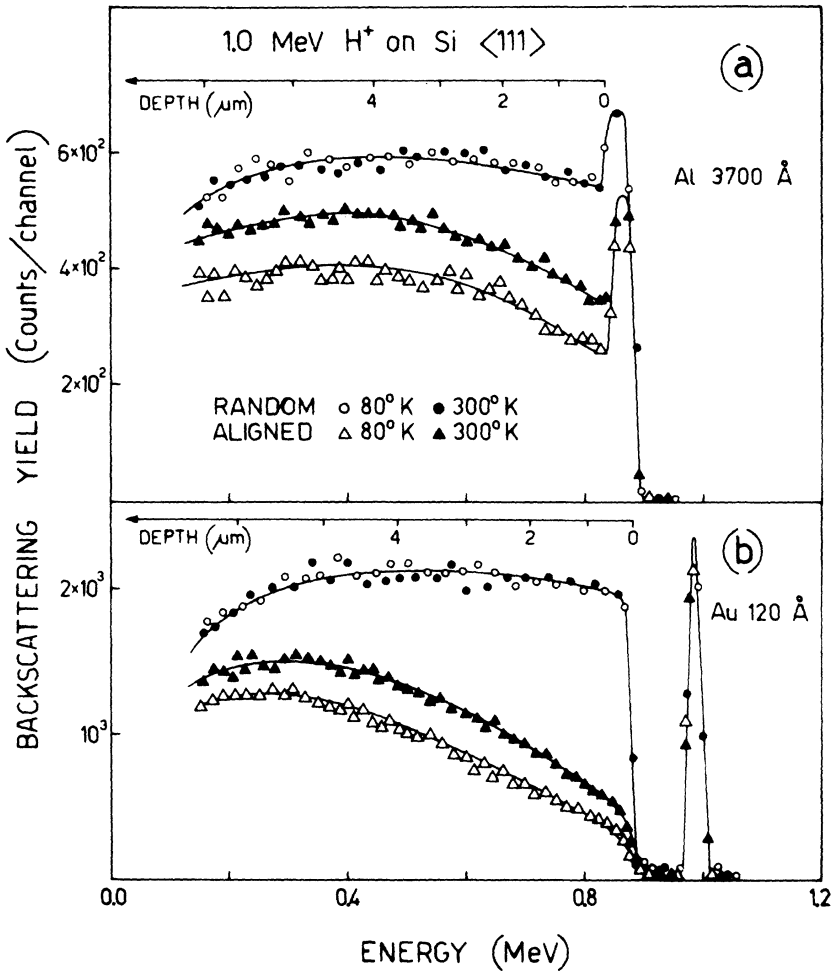

FIG. 1. Energy spectra for 1.0-MeV H^+ backscattered (a) from a silicon crystal covered with 3700 Å of Al for incidence along a random and ⟨111⟩ directions at target temperature of 80 and 300 °K; (b) from a silicon crystal covered with 120 Å of Au for incidence along a random and ⟨111⟩ direction at target temperature of 80 and 300 °K. The top scale in the two figures represents the depth inside the silicon crystal from which the particle has been backscattered.

respectively. The procedure described in Ref. 13 has been adopted to extract the Al signal from the overlap peak between Si and Al.

Figure 1(b) shows three energy spectra of 1.0-MeV H^+ backscattered from silicon covered with 120 Å of Au; on the right-hand side of the figure the signal of the Au layer is visible; on the left-hand side the silicon spectra obtained at random incidence is shown together with two aligned yields for sample temperatures of 80 and 300 °K, respectively. Similar spectra for silicon covered with 3700 Å of Al are shown in Fig. 1(a). In this case, since the film atoms are slightly lighter than the substrate ones, the Si and Al signal overlap producing a peak. In the upper part of the two figures a depth scale is shown for the random spectrum. The energy-to-depth conversion scale has been obtained following the usual procedure[14] from reported stopping powers[15] including energy losses in the films and experimental geometry. The same depth scale has been used for the aligned spectra, and this choice seems reasonable in present measurements because of the spreading produced by

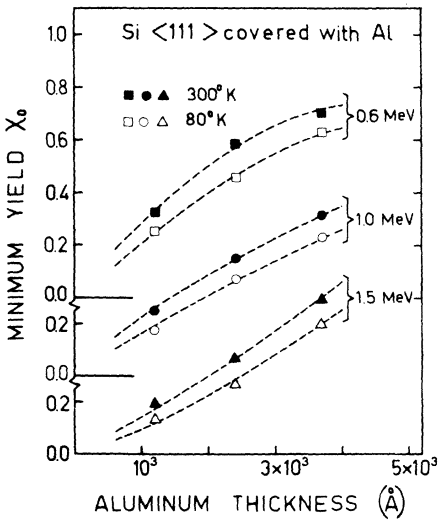

FIG. 2. Minimum yield χ_0 (ratio of aligned to random yield near the surface) vs aluminum layer thickness for 0.6-, 1.0-, and 1.5-MeV H^+ impinging along the ⟨111⟩ axis of covered silicon crystals. The dashed lines are smooth curves through the experimental data.

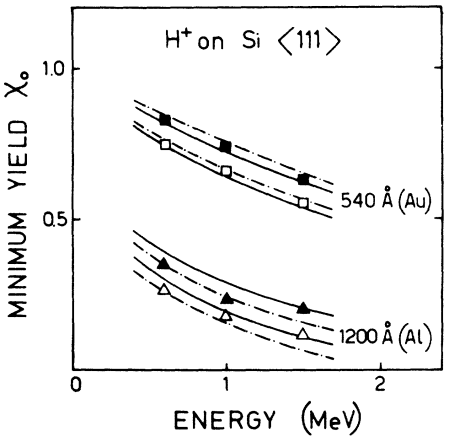

FIG. 3. Minimum yield χ_0 vs beam energy for protons impinging along the ⟨111⟩ axis of silicon covered with 540 Å of Au and with 1200 Å of Al, and for target temperature of 80 °K (△ and □) and 300 °K (▲ and ■). The solid and dashed lines represent the calculated minimum yields by the convolution and steady-increase method, respectively (cf. Sec. III).

the metal layer in the angular distribution of channeled particles. The ratio between the aligned and the random yield at a depth z defines the dechanneled fraction $\chi(z)$. The minimum yield χ_0 is obtained extrapolating to null depth and dechanneled fraction.

III. RESULTS AND CALCULATIONS

A. Aligned to Random Transition

Changes of the minimum yield by varying beam energy, crystal temperature, and film thickness allow, as remarked above, the investigation of the channeled-to-random transition.

The dependence of χ_0 on the film thickness is related to the spreading produced on the beam-particle distribution. The number of particles which enter the crystal with an angle greater than that allowed for channeling increases with film thickness, thus increasing the minimum yield (see Figs. 2 and 3).

For fixed film thickness, χ_0 increases with target temperature. This increase is due to the reduction with temperature of channeling critical angle,[16,17] there being no change in the angular distribution of particles scattered in the amorphous layer.

Also with increasing beam energy the critical angle $\Psi_{1/2}$ decreases, but in this case the scattered-particle distribution becomes narrower; $\psi_{1/2}$ depends[5] on the beam energy E as $E^{-1/2}$, while the angular width changes[8] as E^{-1}. The last factor is then predominant and the net result is a decrease of χ_0 with increasing beam energy.

The minimum yield is determined by (i) the angular distribution $f(\theta)$ of beam particles after traversing the metal layer and the crystal surface and (ii) the probability $Y(\theta)$ that a particle impinging with a given angle moves in a random trajectory.

In formula χ_0 is given by

$$\chi_0 = \int_0^\infty 2\pi\theta\, d\theta f(\theta) Y(\theta) \simeq \int_{\psi_{1/2}}^\infty 2\pi\theta f(\theta) d\theta , \qquad (1)$$

where the last equality holds in the square-well approximation, i.e., in the assumption that the probability $Y(\theta)$ is a step function. The effect of the changes in the distribution and in the critical angle with varying film thickness, beam energy, and crystal temperature are schematically represented, by way of summary, in Fig. 4.

The particle angular distribution just beneath the crystal-surface results, neglecting the experimental angular resolution, from the angular spreading produced by the amorphous layer covering the crystal surface and from the scattering

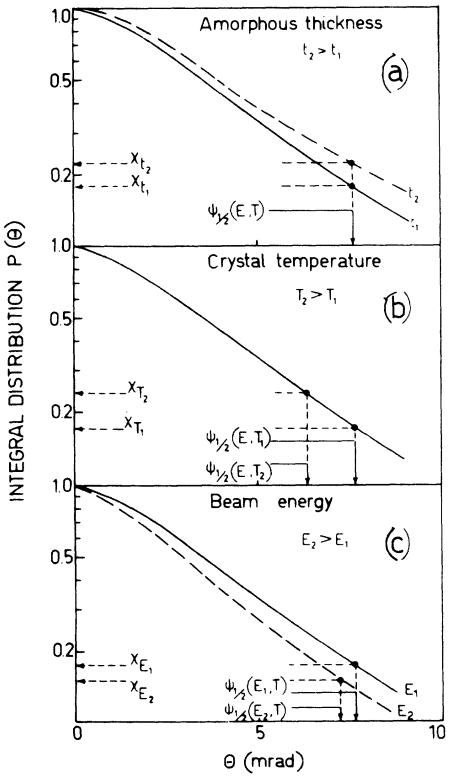

FIG. 4. Schematic diagram of the beam fraction (integral distribution) scattered at angles larger than θ. In the square-well approximation the minimum yield χ_0 is equal to $P(\Psi_{1/2})$, being $\Psi_{1/2}$ the maximum allowed angle for channeling. The figure shows the dependence of $\chi_0 = P(\Psi_{1/2})$ on (a) the amorphous thickness via the beam spreading, (b) the crystal temperature through the variations of the critical angle, and (c) the beam energy which changes both the angular distribution and the critical angle.

due to the lattice potential (transmission factor).[4,5]

The two above kinds of scattering differ in nature. A single event of scattering in the amorphous layer can increase or decrease the particle transverse momentum with respect to a given direction, although the cumulative effect is a beam spreading. The single scattering at the crystal surface instead, always increases the particle transverse energy and hence its transverse momentum by an amount which depends on the entering point. In the following, for a better understanding, not only the angle θ between the particle trajectory and the channel axis but also the transverse momentum $p_\perp = p\theta$ or the transverse energy $E_\perp = E\theta^2$, or the reduced transverse energy[4] $\epsilon_\perp = 2E_\perp / E\psi_1^2$ will be used.

The change in transverse energy due to surface transmission is given by $U(r) - U(r_0)$ where $U(r)$ and $U(r_0)$ are the row potential at a distance r and in the middle of the channel, respectively. Lindhard's[5] standard-row potential has been adopted in the following calculations.

If the particles cross the amorphous layer before entering the crystal, both contributions can be taken into account by adding the corresponding increments of transverse energy. The resulting differential distribution is then

$$p(E_\perp) = \int\int p_a(E_\perp') p_c(E_\perp'') \delta(E_\perp' + E_\perp'', E_\perp)\, dE_\perp' dE_\perp'', \tag{2}$$

where $p_a(E_\perp')$ and $p_c(E_\perp'')$ are the differential distributions produced by the scattering in the amorphous layer and in the lattice potential, respectively. The method used in these calculations is described in detail in Ref. 4.

The film thicknesses give an average number of collisions, within the screening distance, ranging between 1 and 10. In this plural scattering regime the scattered particle distribution depends on the potential which describes the projectile–target-atom interaction. The Thomas-Fermi potential modified by Lindhard and used by Meyer[8] in this treatment of scattering gives good agreement with experimental distributions both in transmission[9,10] and in channeling technique measurements.[6,7] Meyer's treatment of plural scattering has been adopted therefore throughout.

The differential distributions $p(\epsilon_\perp)$ for 1.0-MeV protons after traversing gold layers of different thicknesses entering a {111} surface of Si are shown in the upper part of Fig. 5 as solid lines, where the dashed lines represent the same distributions but without the transmission factor. As one may see, the lattice scattering shifts the peak of the distribution to the right and broadens it. The corresponding integral distributions $P(\epsilon_\perp) = \int_{\epsilon_\perp}^{\infty} p(\epsilon_\perp')\, d\epsilon_\perp'$, i.e., the fraction of beam having a reduced transverse energy greater than $\epsilon_\perp = 2E\theta^2/E\psi_1^2$, are plotted in the lower part of Fig. 5. Their values at $\psi_{1/2}$ give minimum yield in the square-well approximation. The contribution of the transmission factor to minimum-yield values decreases with increasing film thickness falling from 20% for 120-Å to 8% for 540-Å gold layers. In an uncovered crystal, however, the initial distribution is determined by the transmission factor. The presence of an oxide layer or other contamination on the surface can also affect it strongly.

The other factor appearing in Eq. (1) deals with the aligned-to-random transition. Instead of the step-function approximation, it is more reliable to assume, for $Y(\theta)$, the experimental angular yield profile or, as recently proposed,[7] its average over the azimuth angles, both measured near the surface of the uncovered crystal. It may be noted that the experimental yield profiles include the scattering through the crystal surface so that the particle distribution to be used in Eq. (1) must account only for the scattering in the amorphous layer.

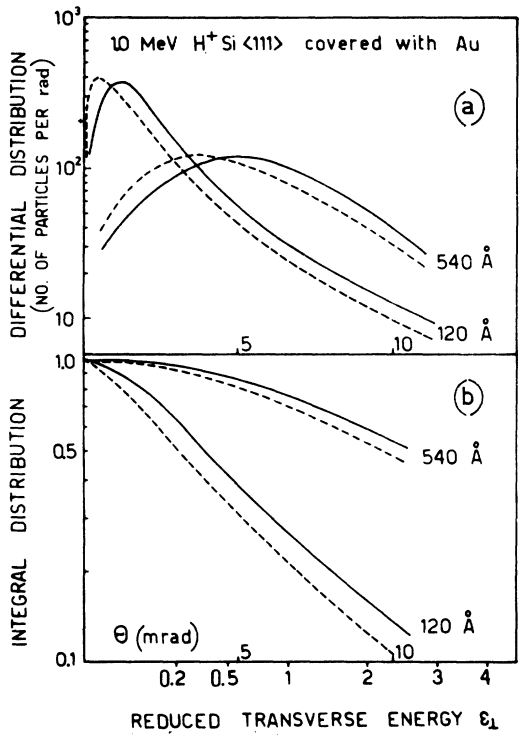

FIG. 5. (a) Number of 1.0-MeV H^+ particles per rad scattered at an angle θ from the initial direction after traversing a thickness of 540 and 120 Å of Au according to Meyer's treatment and neglecting (dashed line) or including (solid line) the scattering through the crystal surface. (b) Integral distribution for the same cases as considered in (a). Two scales are reported in abscissa: θ and the reduced transverse energy $\epsilon_\perp = 2E_\perp/E\Psi_1^2 = 2E\theta^2/E\Psi_1^2$.

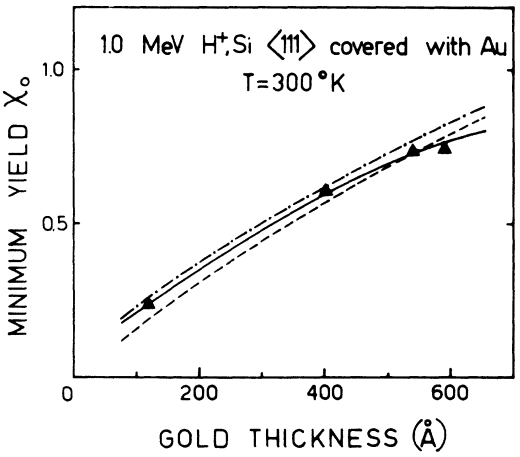

FIG. 6. Minimum yield vs gold thickness for 1.0-MeV H^+ impinging along the ⟨111⟩ axis of silicon target at 300 °K. The calculated values have been obtained in the square-well approximation neglecting (dashed line) or including (dot-dashed line) the transmission factor and by the convolution method (solid line).

The measured χ_0 values are reported in Figs. 2, 3, and 6 by varying the experimental parameters. The values calculated with the angular-yield profile and with the step-function condition either including or neglecting the transmission factor are shown in Figs. 3 and 6. The disagreement between experimental and calculated values of χ_0 ranges within ± 0.05. In a comparison of the different approximations it appears that at low film thickness the initial distribution determines mainly the χ_0 values and then the transmission factor is important; at large film thickness the dechanneling condition prevails instead.

A further support to the choice of the dechanneling condition from experiments is gained by changing the crystal temperature which causes a variation of the angular yield profile and hence of $\psi_{1/2}$; typically from 80 to 300 °K, $\psi_{1/2}$ decreases by about 20%. The corresponding minimum-yield variations depend on the slope of the integral distribution in the range of $\psi_{1/2}$ values (see Fig. 4). These changes are usually a fraction of the minimum yield; in experiments with uncovered crystals where χ_0 is a few percent, the change is, therefore, within the experimental uncertainties. A covered crystal, because of the higher minimum yield, is suitable instead to measure these changes as reported in Figs. 2 and 3.

As shown from all the previous data the minimum yield in a covered crystal can be evaluated in a simple way from the angular distribution of particles scattered in the amorphous layer and from experimental critical angle $\psi_{1/2}$ for channeling. The accuracy of this estimation is of the order of ± 0.07, and the agreement with experimental values can be improved by some factor accounting for the transmission through the surface and for the angular profile.

B. Scattering in the Channel

The increase of the dechanneled fraction $\chi(z)$ with depth z is related to the scattering of the beam particles in the channel. Transitions of particles from the condition of correlated motion inside the channel to the condition of random motion are due to nuclear and electronic multiple scattering which increase the particle transverse energy, i.e., the angle the trajectory forms with the channel axis.

Because the angular distribution of the beam just beneath the crystal surface and the transition probability are known, as discussed above, the experimental dechanneled fraction gives a measure of the scattering experienced by channeled particles.

Calculations of the dechanneled fraction require, in general,[5] the solution of a diffusion equation for the transverse momentum distribution of channeled particles. The diffusion coefficient represents the magnitude of the scattering and it is related to the channel cross section sampled by particles as a function of their transverse momentum. Boundary conditions are given by the initial transverse energy distribution and by the dechanneling transition probability.

This approach has been recently developed[11] and the results have been compared with those of the simpler steady-increase approximation,[4] which allows analytical solutions. The comparison shows that for particles having a very narrow distribution in transverse momentum (δ function), the diffusion smearing becomes dominant with increasing traversed depth. It comes out, however, that the same effect is small if a finite width distribution is considered. This is understood because the diffusion affects much less a smooth distribution than a sharp one. A channeled beam which is scattered at least by the crystal potential at the surface has a distribution wide enough to allow the neglecting of diffusion[18] up to ~10 μm for 1-MeV protons along the main axes of Si.[4,11] In a covered crystal the initial distribution of a channeled beam is wider and the diffusion term further negligible. The steady-increase method has been then applied. In this approximation the increase of the reduced transverse energy with depth can be obtained analytically from

$$\delta\epsilon_\perp = [A_n(E, T) f_n(\epsilon_\perp) + B_e(E) f_e(\epsilon_\perp)]\, \delta z \,, \qquad (3)$$

where the nuclear contribution $A_n f_n$ has been separated from the electron one $B_e f_e$. The values of A_n and B_e and the functions f_n and f_e are reported in detail in Refs. 4 and 18, where the analytical solution of Eq. (3) is also discussed.

The dechanneled fraction $\chi(z)$ versus depth is

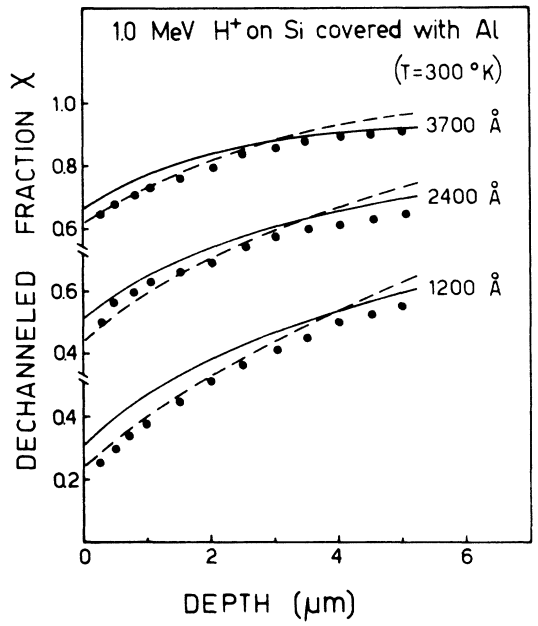

FIG. 7. Experimental and calculated dechanneled fraction χ vs depth for 1.0-MeV H^+ impinging along the $\langle 111 \rangle$ axis of a silicon crystal covered with different thicknesses of amorphous Al. The solid lines represent values calculated by convolution of the differential distribution with the experimental angular yield profiles measured at different depths inside an uncovered crystal. The values calculated in the steady-increase approximation, including the surface transmission, are shown as dashed lines.

determined by (a) the initial integral distribution which includes the scattering in the amorphous and through the crystal surface; (b) the solution of Eq. (3) which accounts for the scattering in the channel; and (c) the dechanneling condition which is assigned in the square-well approximation by the experimental $\psi_{1/2}$. For any transverse energy $\epsilon_\perp$ the solution of Eq. (3) gives the depth z at which the particles that entered with $\epsilon_\perp$ are dechanneled, and the corresponding dechanneled fraction $\chi(z)$ is obtained by the value of the integral initial distribution at $\epsilon_\perp$.

Figure 7 shows the depth dependence of dechanneled fraction measured with 1.0-MeV H^+ impinging along the $\langle 111 \rangle$ axis of Si covered with aluminum layers. Figure 8 reports similar results for 1.5-MeV H^+ and for different crystal temperatures. The dashed lines represent (in both figures) calculated dechanneling curves in the steady-increase approximation just discussed.

Another procedure to compute dechanneled fraction in covered crystal uses, instead of the theoretical description given by Eq. (3), the experimental angular profiles measured at different depths in the uncovered crystal. They give, in fact, the probability of dechanneling for a particle impinging on the crystal with a well-defined incidence angle as a function of the traversed depth in the crystal. A typical depth dependence of the experimental angular yield for an uncovered crystal is shown in Fig. 9. These angular yields include the transmission factor, the scattering in the channel, and the dechanneling condition. The dechanneled fraction for a covered crystal at a given depth is given then by convolution of the initial distribution due only to the amorphous layer with the experimental profile measured at the same depth. This procedure is an extension of the method previously adopted for minimum-yield calculations [cf. Eq. (1) and Sec. III A]. The solid lines reported in Figs. 7 and 8 are the dechanneled fractions obtained by the above empirical method which in all the investigated cases agree very well with the experimental values. This result supports further the Meyer's plural scattering treatment. The curves calculated in the steady-increase approximation (dashed lines) show a good agreement for thicker layers, while some disagreement occurs for very thin films. These discrepancies, consistent with previous results[4,12,18] in uncovered crystals, are due to neglecting the effect of diffusion on the transverse momentum of the channeled beam. With increasing amorphous thickness the initial distribution spreads out and the diffusion effect becomes less relevant.

C. Determination of Scattered Particle Distribution

The dechanneling in a covered crystal has been considered so far by a description of the scattering events in a known amorphous layer and in the channel. The agreement found between experiments and calculations supports both Meyer's treatment of plural scattering in the amorphous layer and the steady-increase approximation for the channel scattering.

The same agreement, on the other hand, allows, by a reverse procedure, a direct evaluation of the scattered particle distribution in an amorphous layer or in a heavy disordered region. The aim consists then in obtaining from the measured dechanneled fraction the distribution of scattered particle and then, e.g., the thickness of the disordered region. This can be accomplished by one of the two above approaches, i.e., either adopting the steady-increase approximation or using the experimental angular profiles measured as a function of depth in the uncovered crystal.

The first procedure is illustrated in Fig. 10 which reports the measured dechanneled fraction $\chi(z)$ versus depth and the depth $z(\epsilon_\perp)$, given by Eq. (3), at which a particle having an initial transverse energy $\epsilon_\perp$ is dechanneled. The right-hand side represents the initial integral distribution

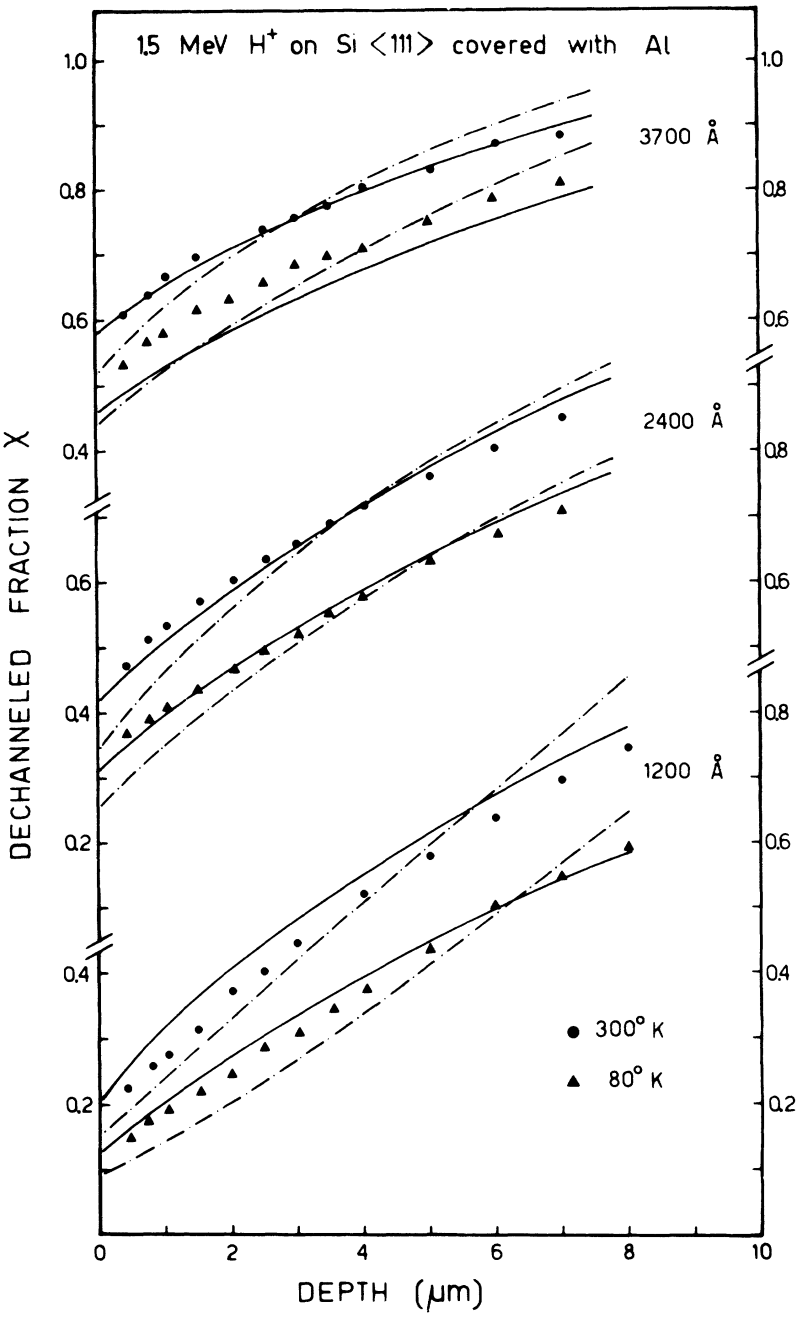

FIG. 8. Experimental calculated dechanneled fraction χ vs depth for 1.5-MeV H^+ impinging along the $\langle 111 \rangle$ axis of silicon covered with different thicknesses of amorphous Al and for target temperature of 80 and 300 °K. The solid and dashed lines represent the fraction values calculated by the convolution and steady-increase method, respectively.

$P(\epsilon_\perp)$ found by eliminating z from the two above functions as shown by the arrows. In this case the obtained distribution accounts for the scattering in the amorphous layer and through the crystal surface.

The deconvolution of the experimental dechanneled fraction using the angular yield profiles taken at different depths inside the uncovered crystal gives instead the distribution of particles scattered by the amorphous layer only. This distribution differs from that obtained with the steady-increase method because it does not account for the transmission factor which is already included in the experimental angular yield profile. For simplicity, the experimental profiles of the uncovered crystal have been approximated by a step function as in Fig. 9, whose width $\psi_{1/2}(z)$ and dip $[1-\chi(z)]$ decrease with traversed depth. The deconvolution can then be carried out with respect to the integral distribution P by solving the following equation:

$$\chi_c(z) = P(\psi_{1/2}(z)) + [1 - P(\psi_{1/2}(z))]\chi_u(z), \qquad (4)$$

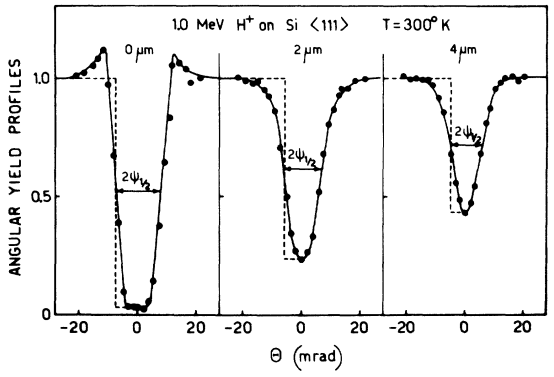

FIG. 9. Depth dependence of the experimental angular yield profiles for 1.0-MeV H^+ impinging around the ⟨111⟩ axis of an uncovered silicon target.

where $\chi_c(z)$ is the measured dechanneled fraction in the covered crystal; $\psi_{1/2}(z)$ and χ_u are, respectively, the half-width at half-dip and the dechanneled fraction both measured in the uncovered crystal; P is the initial integral distribution as a function either of the angle $\psi_{1/2}(z)$ with the channel

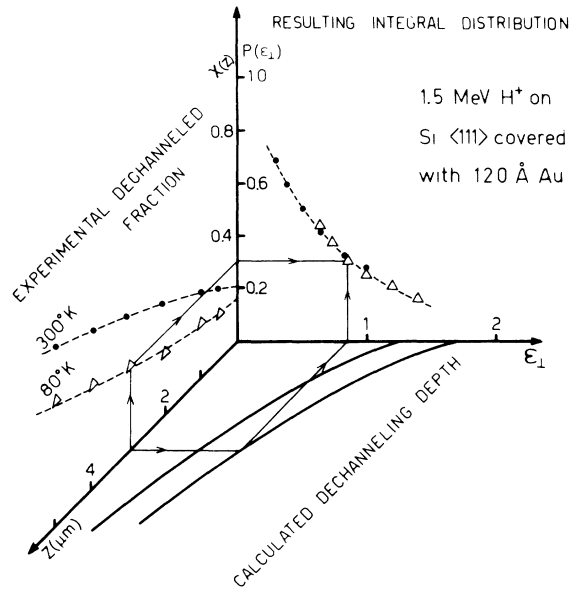

FIG. 10. Graphical determination of the integral distribution from the experimental dechanneled fraction and from the computed depth $z(\epsilon_\perp)$ at which a particle of an initial reduced transverse energy $\epsilon_\perp$ reaches the critical value $\epsilon_\perp^* = 2E\Psi_{1/2}^2/E\Psi_1^2$ to be dechanneled. The data refer to 1.5-MeV H^+ impinging along the ⟨111⟩ axis of silicon covered with 120 Å of Au and for target temperature of 80 and 300 °K. Entering at a given depth z the resulting $P(\epsilon_\perp)$ value is equal to the corresponding experimental dechanneled fraction $\chi(z)$, while the $\epsilon_\perp$ value is obtained from the computed dechanneling depth $z(\epsilon_\perp)$ (follow the arrows).

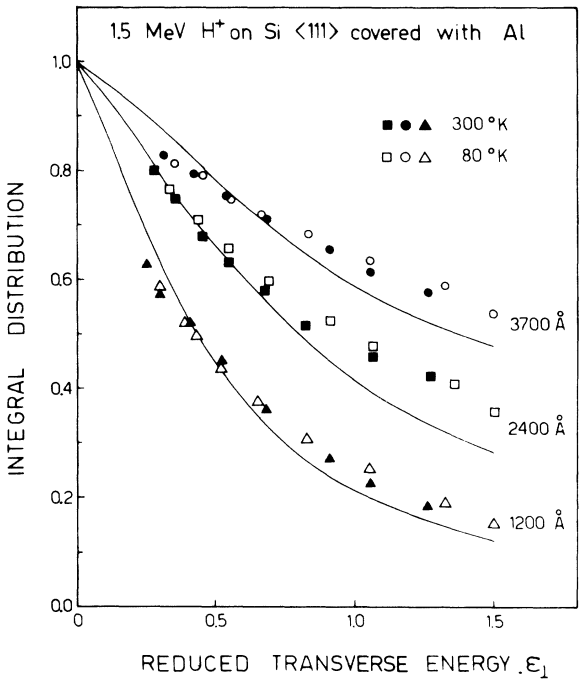

FIG. 11. Resulting integral distributions, obtained by the experimental dechanneled fraction and the calculated dechanneling depth (see Fig. 10) for 1.5-MeV H^+ on ⟨111⟩ axis of silicon covered with Al, are compared with those calculated.

axis or of the reduced transverse energy $\epsilon_\perp = 2E_\perp / E\psi_1^2 = 2\psi_{1/2}^2(z)/\psi_1^2$.

The integral angular distribution of scattered particles using the steady-increase approximation is plotted as the points in Figs. 11 and 12 as a function of the reduced transverse energy for different thicknesses of aluminum and gold films. The theoretical distributions calculated including both the scattering in the amorphous layer (Meyer's treatment) and through the crystal surface are shown in the same figures as solid lines. The thickness of the amorphous layer to compute theoretical distribution has been measured by helium backscattering (see Sec. II). As it appears from the figures the agreement between theoretically and experimentally determined curves is quite good, and the thickness can be evaluated within 10%.

Two integral distributions obtained by the deconvolution method [i.e., by solving Eq. (4)] are reported in Fig. 13, where for comparison the corresponding distributions given by the steady-increase method and already shown in Fig. 11 are also plotted. These two sets of results differ for the transmission factor which is included in the distributions obtained in the steady-increase approach while it is taken off in those given by the deconvolution procedure. The corresponding theo-

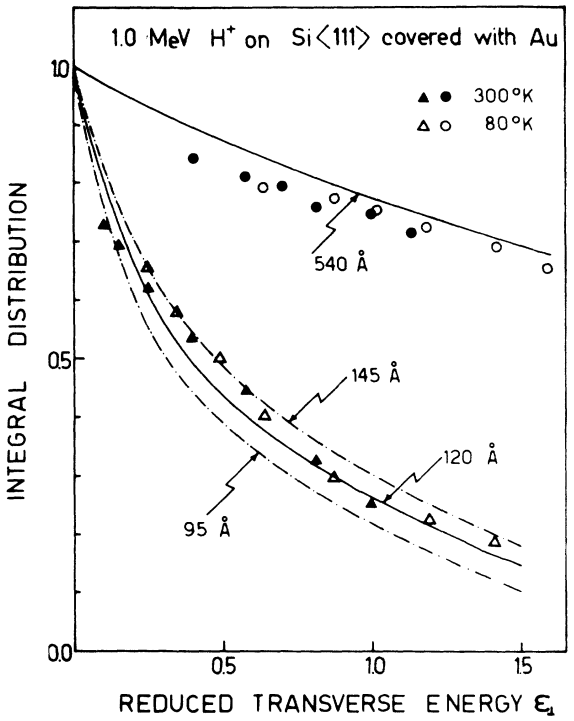

FIG. 12. Resulting integral distributions, obtained by the experimental dechanneled fraction and the calculated dechanneling depth for 1.0-MeV H^+ entering along the ⟨111⟩ axis of silicon covered with Au, are compared with those calculated.

retical curves to compare with have been computed then with or without the transmission factor.

The measured dechanneled fractions, the angular yield profile, and the solution of Eq. (3) all depend on the crystal temperature, while the scattering in the amorphous layer and through the crystal surface are independent of it. It should be noted that Figs. 10–12 show that experimental angular distributions obtained under conditions differing only in target temperature coincide with each other. This result is in agreement with the temperature independence of the scattering in the amorphous layer and through the crystal surface.

The comparison between distributions obtained by the deconvolution approach and those provided by the steady-increase method clearly shows the influence of the transmission factor in determining the resulting distribution for low film thickness.

As a prelude to the application of the two above-described procedures to disorder studies the following remarks should be made. A heavy damaged crystal, i.e., a crystal region with a large density of defects which destroy the atomic arrangement, can be investigated either by means of deconvolution procedure or by the steady-increase approach. The first method requires measurements both in the undamaged and in the damaged crystal, while the latter implies the solution of Eq. (3), i.e., the treatment of the scattering experienced by a channeled particle in the undamaged crystal.

In a crystal with low disorder concentration and distributed defects, however, the deconvolution method cannot be applied because it requires a perfect crystal where particles move after traversing the damaged region. The steady-increase procedure is, instead, suitable because one can account for the scattering produced by simple defect in the channel on the same basis adopted in treating thermal vibrations and electronic distribution. Formally, this requires the addition of an extra contribution to the right-hand side of Eq. (3), which should depend on the location and on the nature of defect and on the type, energy, and transverse energy of the moving particle.

IV. SUMMARY AND CONCLUSIONS

The minimum yield χ_0 and the depth dependence of the dechanneled fraction $\chi(z)$ have been measured in silicon overlaid with aluminum and gold evaporated layers as a function of proton beam en-

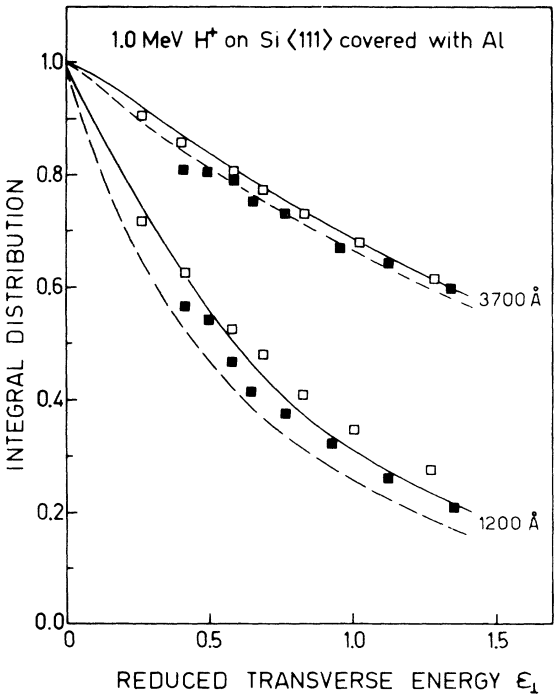

FIG. 13. Resulting integral distributions obtained by the steady-increase method (□) and by the deconvolution of the experimental dechanneled fraction with the angular yield profile measured at different depths inside an uncovered crystal (■). The two sets of results differ for the transmission factor which is included in the steady-increase approach. The experimental results are compared therefore with Meyer's distribution (dashed line) and with the same including the crystal-surface transmission (solid line).

ergy, crystal temperature, and film thickness.

The minimum yield χ_0 has been computed by convolution of the Meyer's angular distributions for the scattering in the amorphous layer with either the angular-yield profile measured near the surface of the uncovered crystal or a square-well approximation to this profile. The simplest method which neglects the crystal-surface transmission and uses the step-function approximation gives the χ_0 values within $\pm 5\%$ of the random value. It must be remarked that at low film thickness the crystal surface transmission affects appreciably the initial distribution and then the minimum yield.

The dechanneled fraction $\chi(z)$ has been calculated also by the convolution method, but taking the angular yield profiles measured at different depths inside an uncovered crystal. Alternatively the steady-increase approximation for the scattering experienced by a particle in a channel has been used with the initial distribution which accounts for the scattering in the amorphous surface layer and through the crystal surface. The dechanneled fractions calculated either by the convolution or by the steady-increase method agree with experimental values within a few percent and they reproduce well the depth dependence. Both methods, can be used in a reverse way to obtain from the measured dechanneled fraction the distribution of particles scattered by an unknown amorphous layer or by an heavily damaged region. This aspect has been investigated as a prelude to disorder determination. The experimental integral distribution, obtained by analysis of the dechanneled fractions with the steady-increase method, agree with the theoretical ones within 10–20%, allowing the thickness of the amorphous layer to be evaluated with the same accuracy (see Fig. 12).

Because a similar accuracy is achieved by the deconvolution procedure, the last is more suitable for its simplicity to treat an amorphous layer or a heavily damaged region. For a small concentration of defects distributed inside the crystal the last method cannot be applied because it is based on an over-all description of the scattering processes as it results from the experimental angular yield profiles. The steady-increase method, however, uses a detailed description of the scattering processes and it seems then more powerful and suitable for treating also distributed defects.

ACKNOWLEDGMENTS

Discussions with E. Lugujjo and J. W. Mayer are acknowledged. Thanks are due to V. Scuderi for the cooperation in performing the experiments.

---

*Supported in part by Centro Siciliano di Fisica Nucleare e di Struttura della Materia and by Gruppo Nazionale di Struttura della Materia del Consiglio Nazionale delle Richerche.

[1]J. W. Mayer, L. Eriksson, and J. A. Davies, *Ion Implantation in Semiconductors* (Academic, New York, 1970), Chap. 3.
[2]S. T. Picraux, Appl. Phys. Lett. **20**, 91 (1972).
[3]E. Bøgh, Can. J. Phys. **46**, 653 (1968); L. C. Feldman and J. W. Rodgers, J. Appl. Phys. **41**, 3776 (1970); J. W. Westmoreland, J. W. Mayer, F. H. Eisen, and B. Welch, Radiat. Eff. **6**, 161 (1970); J. E. Westmoreland, thesis (California Institute of Technology, Pasadena, Calif. 1971). (unpublished); J. F. Ziegler, J. Appl. Phys. **43**, 2973 (1972).
[4]G. Foti, F. Grasso, R. Quattrocchi, and E. Rimini, Phys. Rev. B **3**, 2169 (1971).
[5]J. Lindhard, K. Dan. Vidensk. Selsk. Mat.-Fys. Medd. **34**, No. 14 (1965).
[6]E. Rimini, E. Lugujjo, and J. W. Mayer, Phys. Rev. B **6**, 718 (1972).
[7]E. Lugujjo and J. W. Mayer (unpublished).
[8]L. Meyer, Phys. Status Solidi B **44**, 253 (1971).
[9]F. Bernhard, J. Lippold, L. Meyer, S. Schwalse, and R. Stolk, in *Atomic Collision Phenomena in Solids*, edited by D. W. Palmer, N. W. Thompson, and P. D. Townsend (North-Holland, Amsterdam, 1970), p. 663.
[10]H. H. Andersen and H. Bøttiger, Phys. Rev. B **4**, 2105 (1971).
[11]E. Bonderup, H. Esbensen, J. U. Andersen, and H. E. Schiøtt, Radiat. Eff. **12**, 261 (1972).
[11]F. Grasso, in *Channeling in Solids*, edited by D. V. Morgan (Wiley, New York, 1973).
[13]I. V. Mitchell, M. Kamoshida, and J. W. Mayer, J. Appl. Phys. **42**, 4378 (1971).
[14]J. A. Davies, J. Denhartog, and J. L. Whitton, Phys. Rev. **165**, 345 (1968).
[15]G. Williamson and J. P. Boujot, Commissariat a l'Energie Atomique Report No. CEA 2189, 1962 (unpublished).
[16]J. U. Andersen and E. Uggerhøj, Can. J. Phys. **46**, 517 (1968).
[17]S. U. Campisano, G. Foti, F. Grasso, I. F. Quercia, and E. Rimini, Radiat. Eff. 13, 23 (1972).
[18]S. U. Campisano, F. Grasso, and E. Rimini, Radiat. Eff. **9**, 153 (1971).